

Phase growth in amorphous Si-Cu system: combination of SNMS, XPS, XRD, 4W resistance techniques

Bence Parditka

PhD student

Aix-Marseille Université, IM2NP,
Faculté des Sciences de Saint-Jérôme,
case 142, 13397
Marseille, France

Department of Solid state physics
University of Debrecen
Debrecen, Hungary



Solar cells (c-Si ~ 90%)

- ➔ Physical vapor deposited thin Si films are usually amorphous
- ➔ Recrystallization temperature
- ➔ Metal Induced Crystallization (MIC) (e.g.: bond weakening)

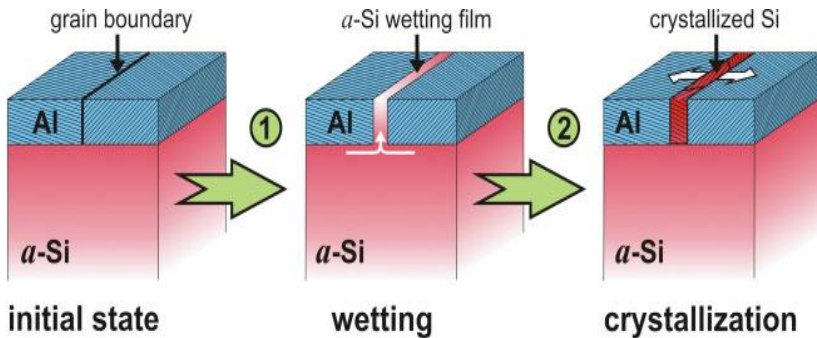


(Fig. 3. Metal Induced Crystallization through GBs in Al-Si system)

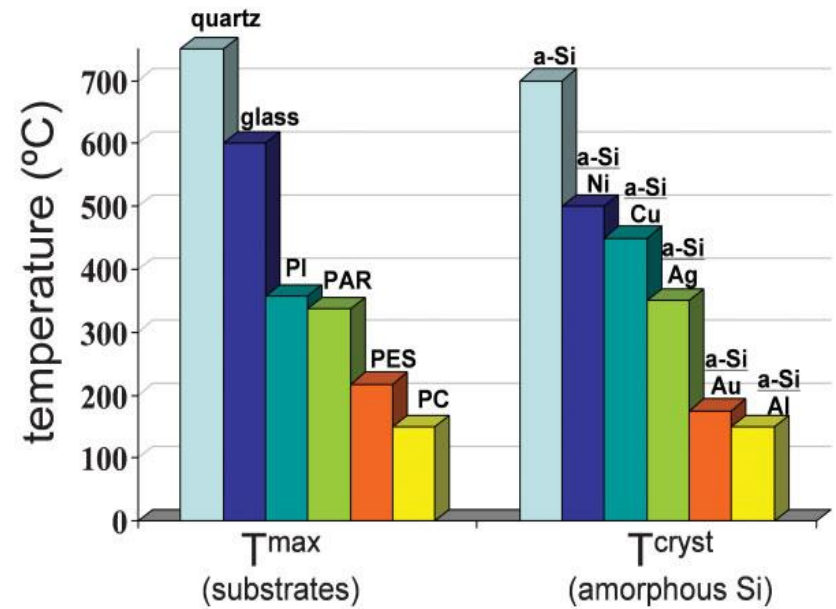
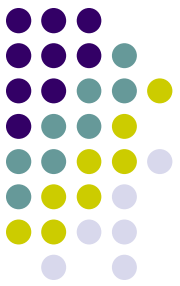


(Fig.2. The left-hand side shows the maximum operating temperatures (T_{max}) of some technologically important substrates: quartz glass, conventional glass, polyimide (PI), polyarylate (PAR), polyethersulfone (PES), and polycarbonate (PC). The right-hand side shows the reduction in the crystallization temperature of a-Si (T_{cryst}) induced by contact with various metals.)

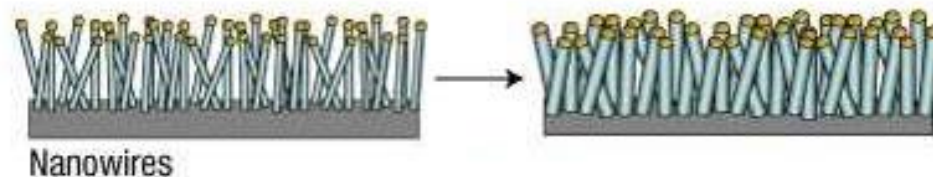
Fig. 1. <http://www.mechanicalengineeringblog.com/tag/silicon-solar-cells/>

Fig. 2., 3. Zumin Wang, Lars P. H. Jeurgens, Jiang Y. Wang and Eric J. Mittemeijer; ADVANCED ENGINEERING MATERIALS 2009, 11, No. 3



Li-ion Batteries

- ⇒ Silicon is more attractive because it has the highest known theoretical specific mass capacity.
- ⇒ Si nanowires - large inherent volume change (400%) during insertion and extraction of lithium.
Results: pulverization and fast capacity fading.
- ⇒ Cu coated Si nanorods / Si-Cu co-deposited nanorods.
Results: higher initial coulombic efficiency, better cycling stability, suppressed pulverization / more flexible, stable nanorods.
- ⇒ Cu₃Si coating (proved by XPS, XRD).



(Fig. 4. Nanowires)

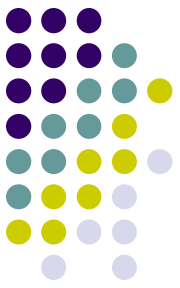
Fig.4. - <http://www.trendhunter.com/trends/stanford-silicon-nanowires-40-hour-laptop-batteries#!/photos/13138/1>

H. Chen et al. / Journal of Power Sources 196 (2011) 6657–6662

M. Au et al.; Journal of Power Sources 196 (2011) 9640– 9647



- ⇒ Cu forms Multiple silicide phase
- ⇒ MIC process starts with the Cu_3Si phase
- ⇒ Studying the phase growth of Cu_3Si has a great importance for applications
- ⇒ We investigated the very early stages of the Cu_3Si growth by combined experimental techniques



Cu/Si bilayer were deposited by magnetron sputtering by a purpose built DC magnetron sputtering device at ambient temperature.

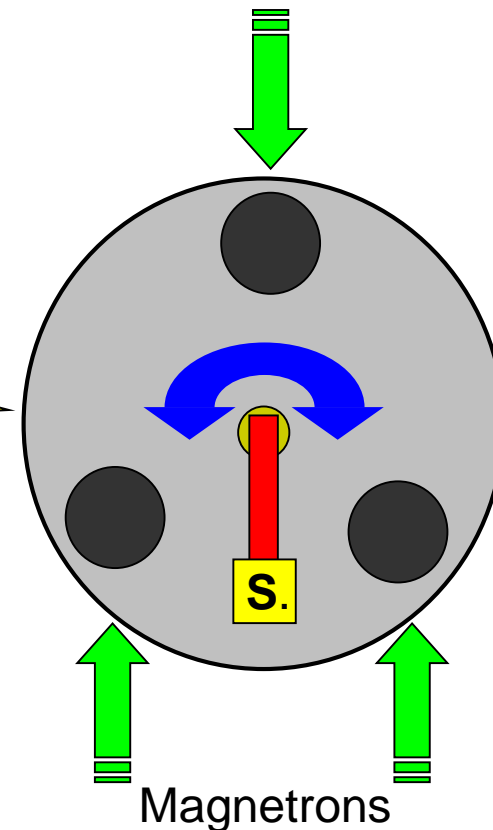


(Fig. 5/b – Magnetron Sputtering System)

(Fig. 5/a – Magnetron Sputtering System)

⇒ The base pressure in the main chamber was 5×10^{-7} mbar.
Cu(99,99%) and Si(99,999%) targets

⇒ The sputtering was performed under the dynamic flow of Ar(99.999%) at a pressure of 5×10^{-3} mbar and the sputtering power was 40W

⇒ All specimens were cut into half. One part of them was kept as prepared while the other could be annealed.

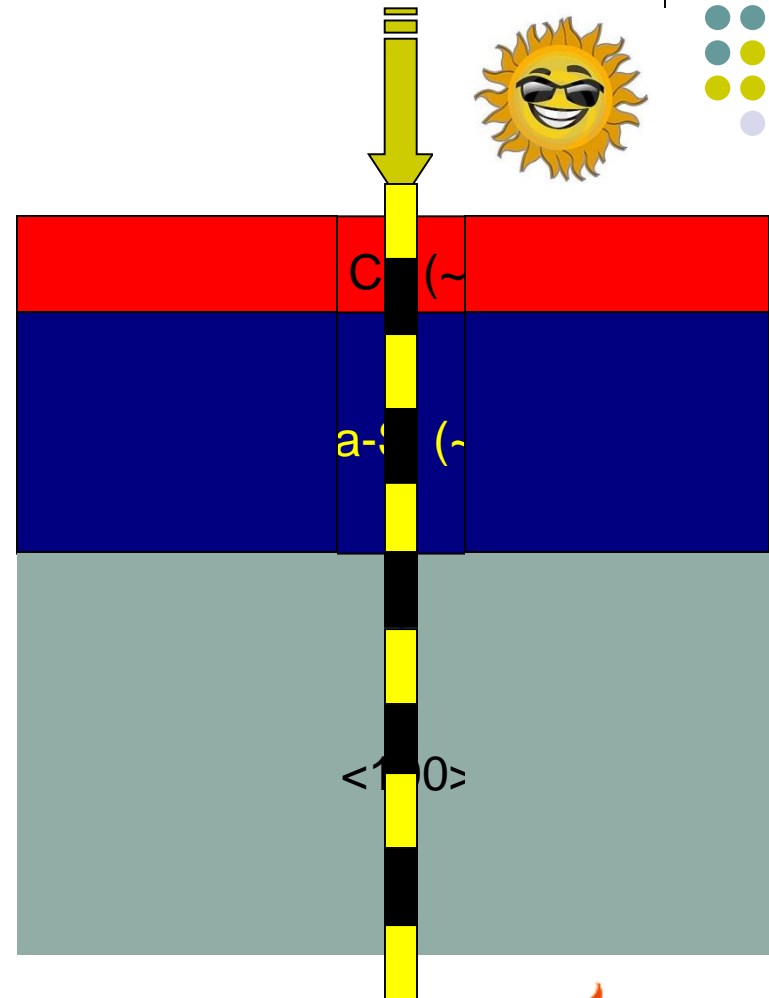


(Fig. 6. – Cu/a-Si/Si<100> substrate sample structure)



SNMS



- ⇒ **S**econdary **N**eutral **M**ass **S**pectrometer - Where the sputtered particles themselves are detected by a mass spectrometer.
- ⇒ The emission and the ionization of the particles, which ones will be detected in the SNMS, separated. Our system uses low-pressure radio frequency plasma for the ionization and the sputtering just as well.
- ⇒ We can obtain information about the elemental composition and the depth profile of our sample.
- ⇒ Because of the destructive nature of the SNMS analysis a separate specimen was required for each analysis.

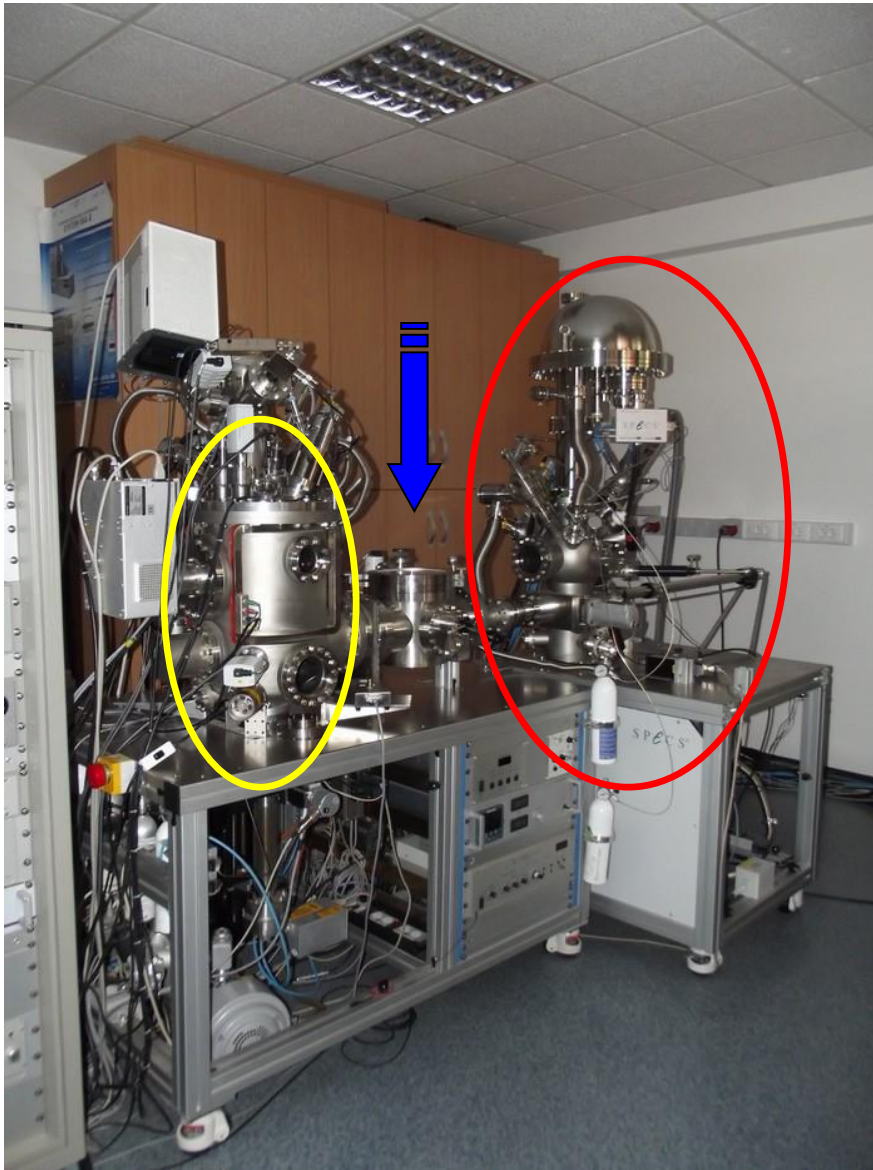


(Fig. 7/a – SNMS and XPS combined system)

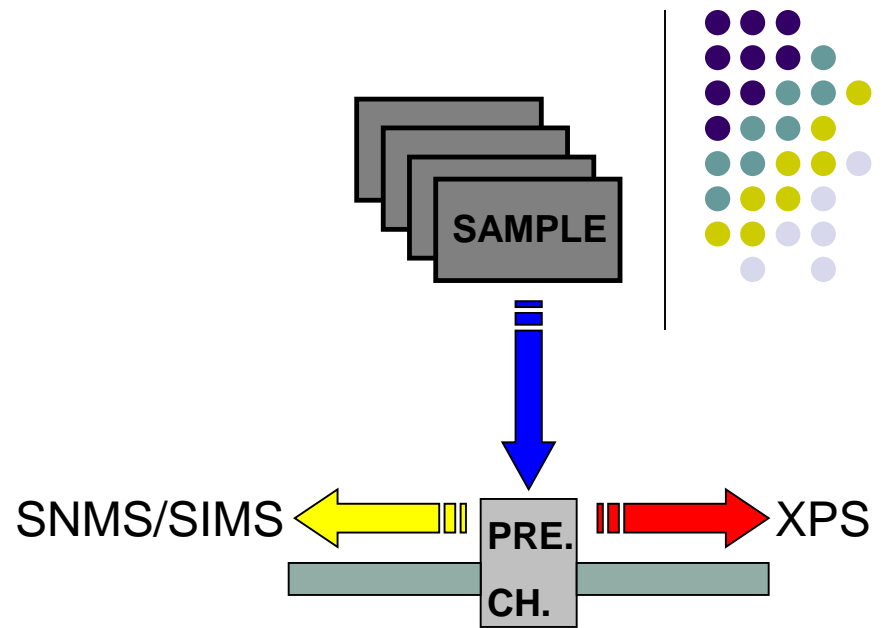


(Fig. 7/b. – schematic figure of the combined SNMS and XPS system)

- ⇒ Multiple sample can be placed in the pre-vacuum chamber. (annealed / as-prepared) – same conditions
- ⇒ In situ XPS measurements after etching.
- ⇒ The samples can be moved from the SNMS into the XPS directly through a pre-vacuum chamber. 8



⇒ The sputtering rates, the deposited thickness of the Cu layer and the new grown phase were determined by an AMBIOS XP-1 profilometer.

⇒ For determining the exact thickness of the deposited layer we used the SNMS in realtime mode in which case the etching were stopped manually at the time when the intensity of Cu and the Si became equal, denoting the interface.

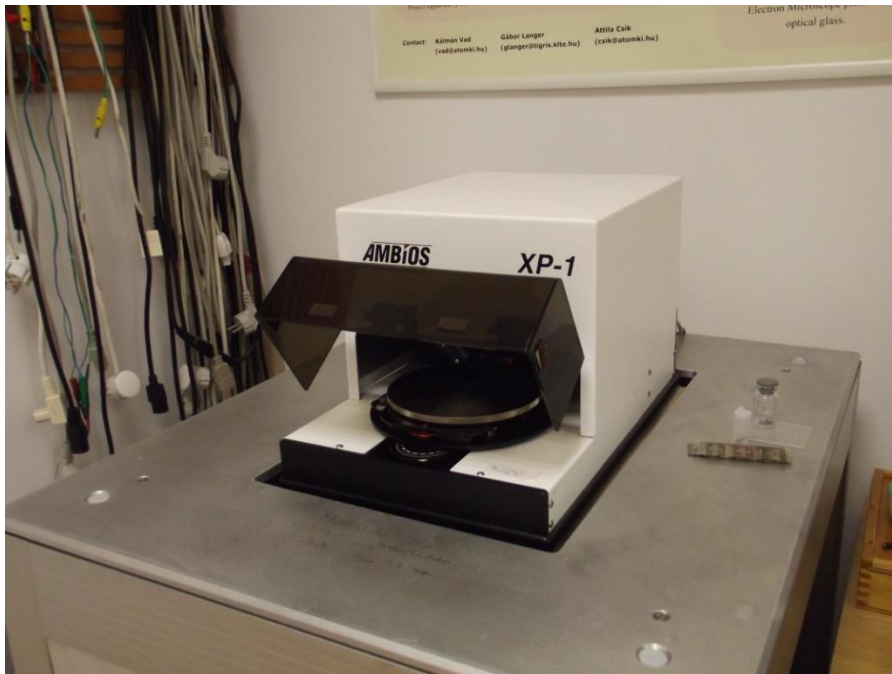


(Fig. 8. – Amibios XP-1 profilometer)

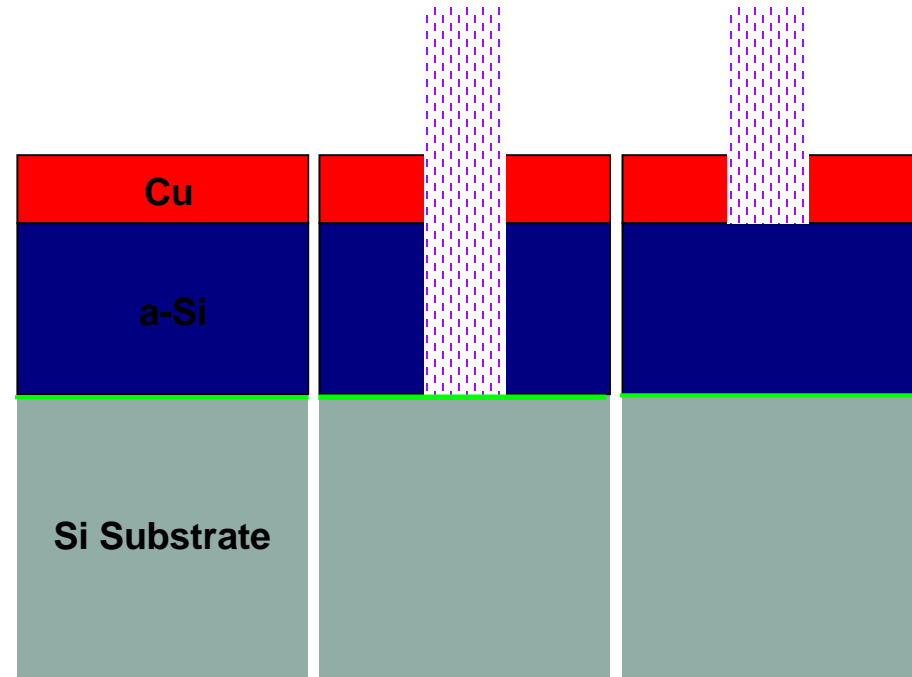


(Fig. 9. – schematic picture of the deposited structure and its thickness determination)



The Cu/Si transition was found to be sharp and this point was set as the position of the original Cu/Si interface.

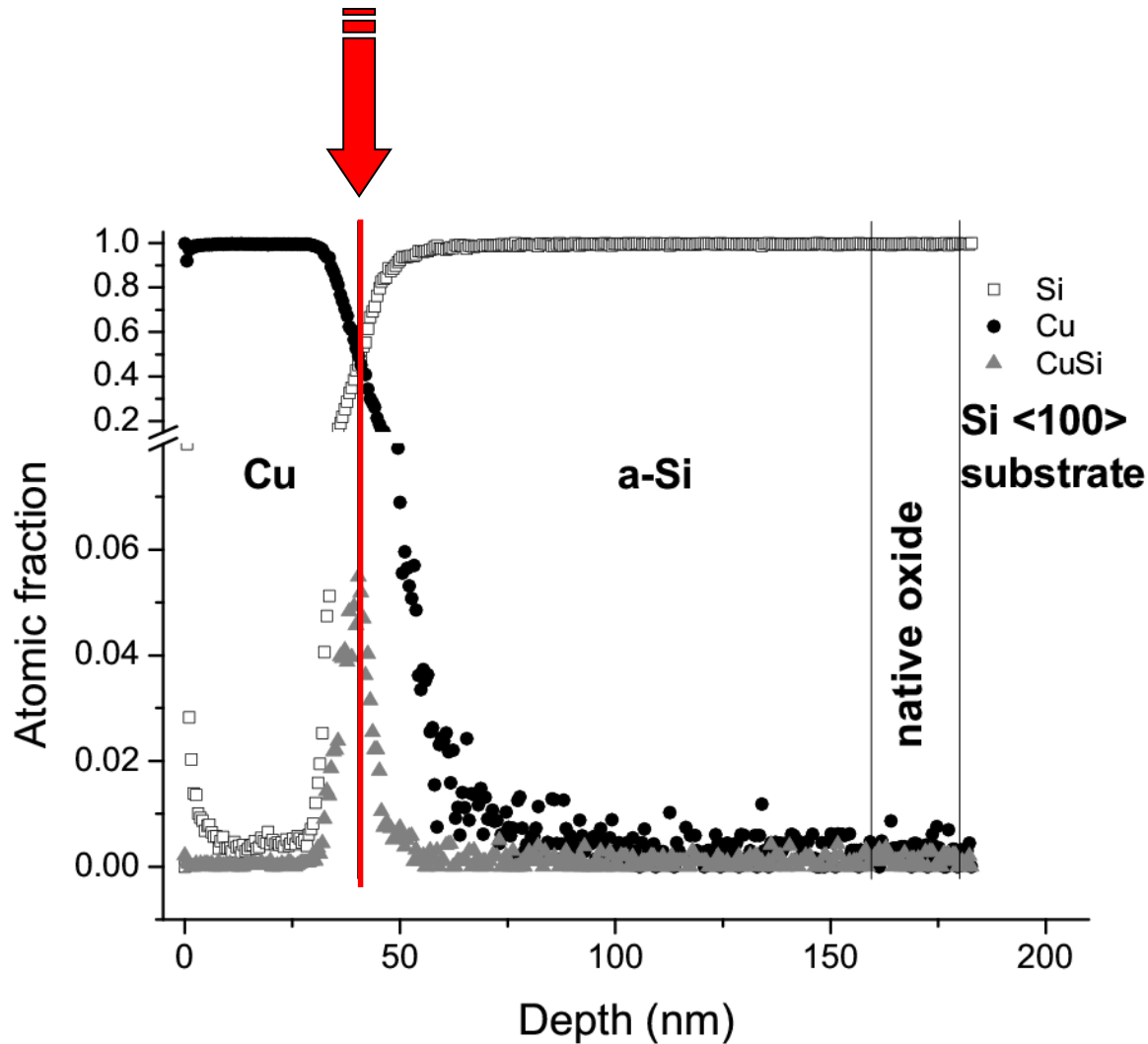


(Fig. 11. – Depth profile of an as-deposited sample)

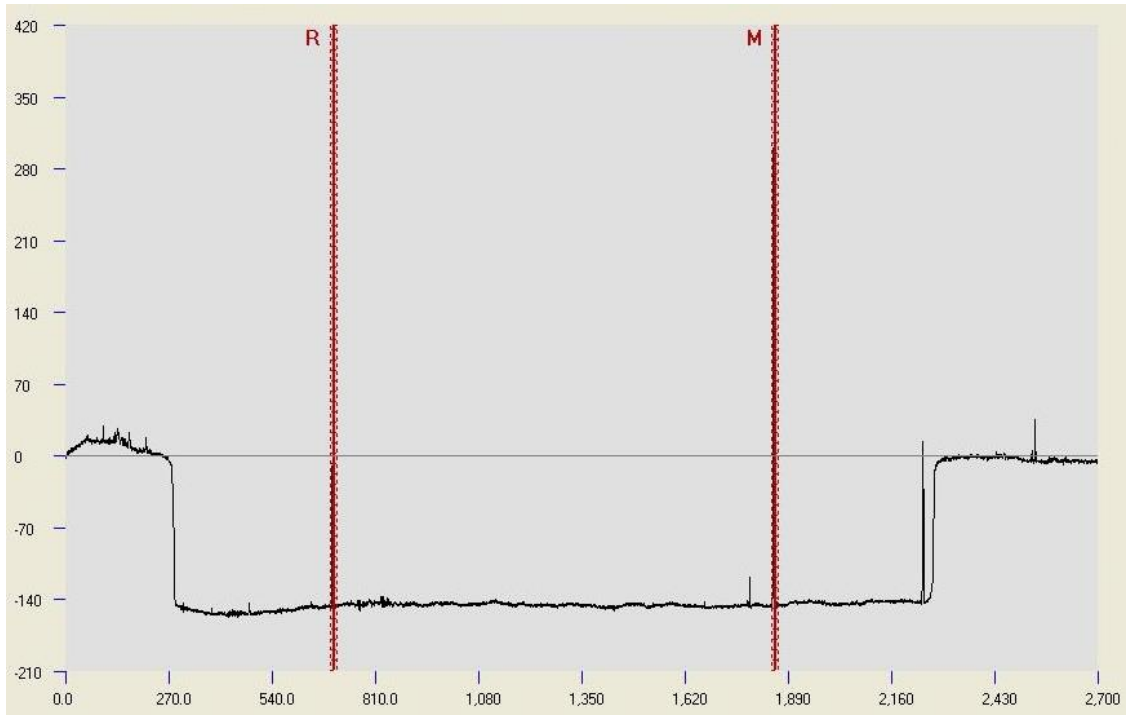


(Fig. 10/a. – linear scan of the profilometer after etching by SNMS)

The measurements with the profilometer were performed in several different angles and at least at two points of the craters to gain an averaged value for the depth in each case.

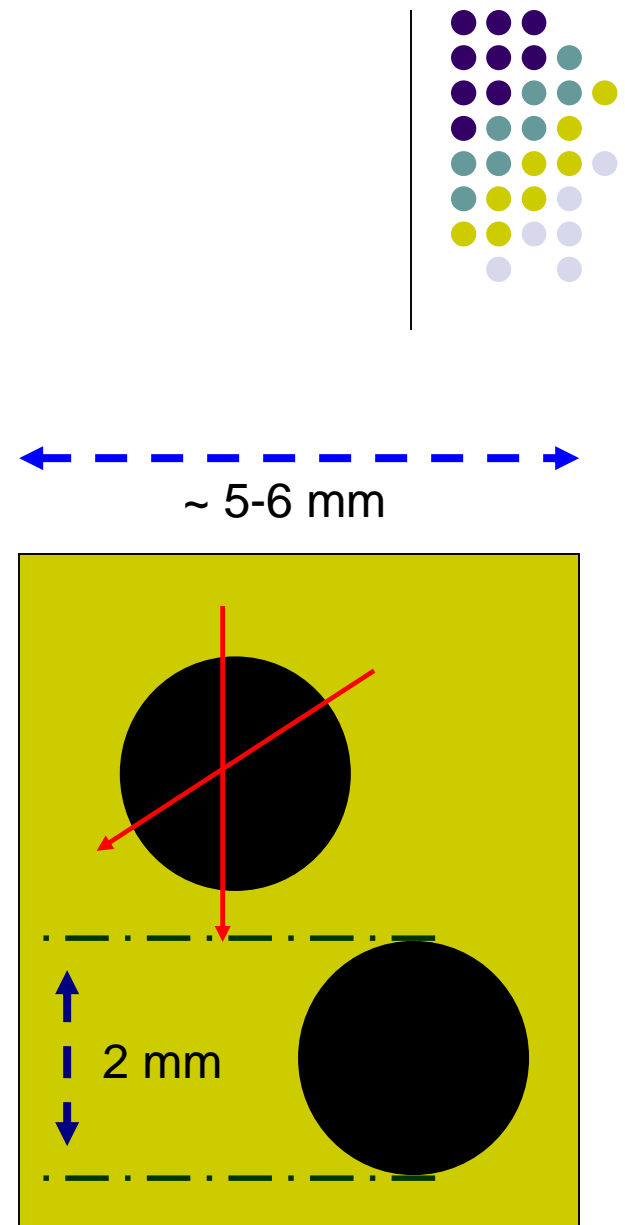
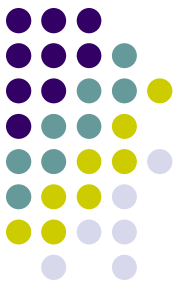


(Fig. 10/b. – The schematic orientation of linear scans of the profilometer and the arrangement of etching by SNMS)



- ⇒ Before the heat treatments resistivity measurements were performed at 408K and 463K under high vacuum (single crystalline sapphire substrates).
- ⇒ We used these samples for XRD investigation too to identify the reaction product. XRD patterns were taken both before and after the annealing treatments.
- ⇒ Heat treatments of 1, 2, 4, 8, 12 and 18 hours at 408 K were carried out (3x) under high vacuum (lower than 4×10^{-6} mbar)
- ⇒ XRD measurements identified that the growing phase is Cu_3Si .

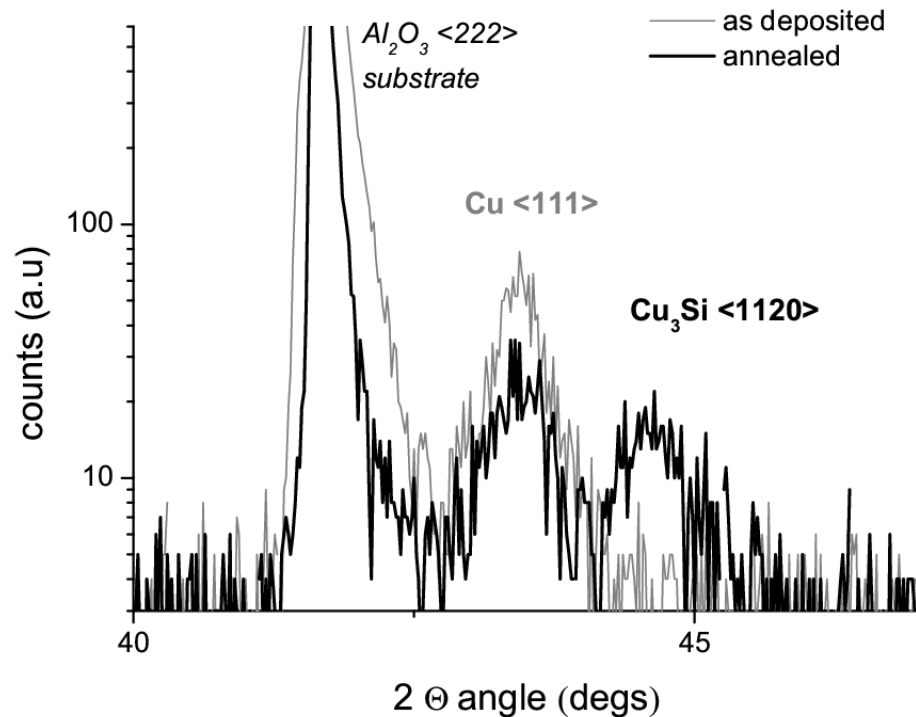
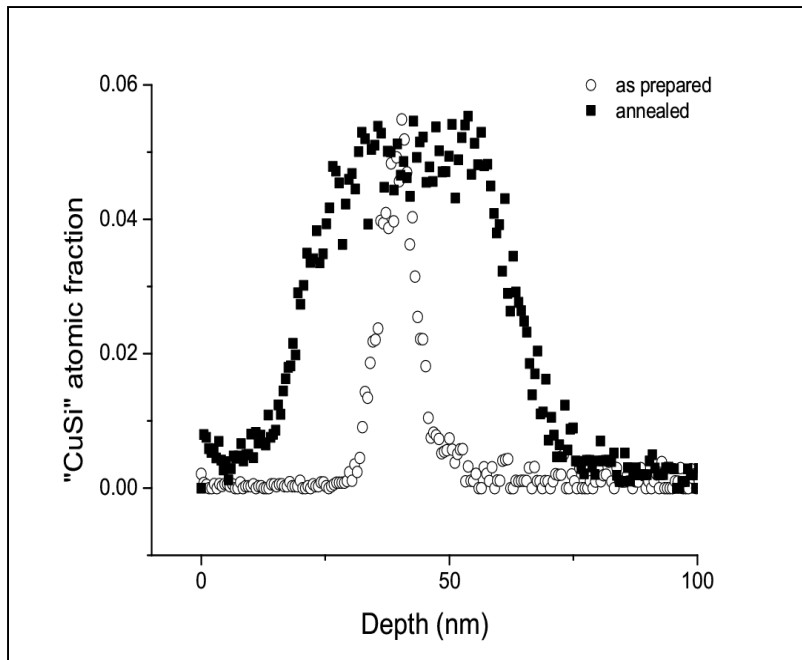
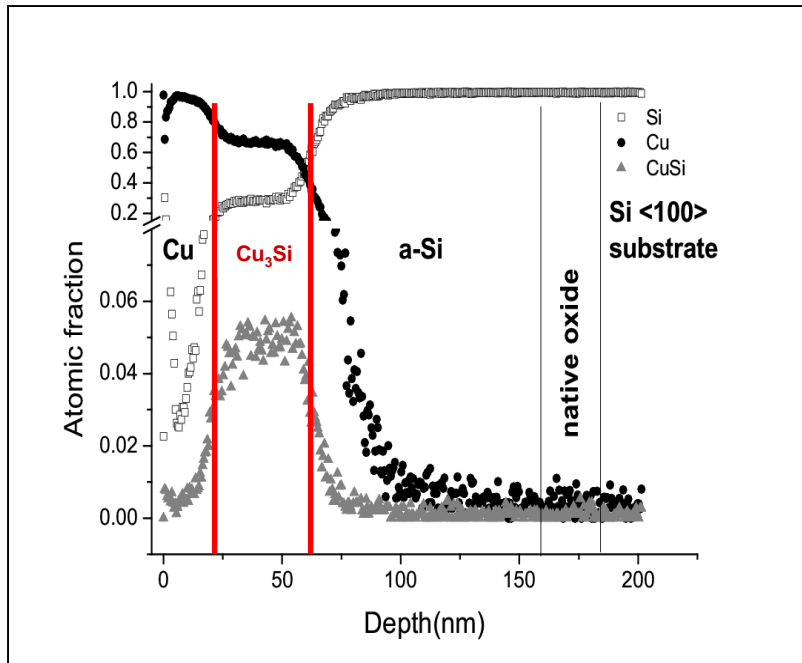


(Fig. 13. – XRD measurement results before and after heat treatment.)



In order to determine the top and bottom positions of the broadening interface the ion bombardment were stopped at the position when the CuSi intensity curve dropped to the half as compared to that of the reaction layer. The CuSi signal was adequately flat in the reaction layer itself.

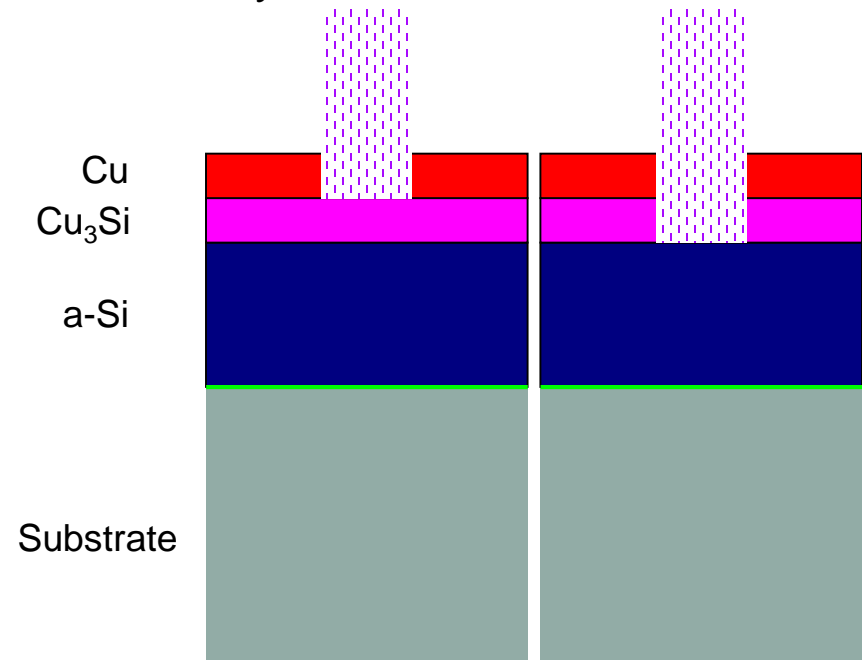


(Fig. 12/a (up), b (down). – SNMS profiles of an annealed sample and Fig. 12/c. – Schematic figure of the etching process)

XPS (Specs)



⇒ (**X**-ray **P**hotoelectron **S**pectroscopy) spectra had been recorded in the pure Cu layer, at the interface of the as-deposited samples and compared to those recorded at the product layer in the annealed counterpart samples. These showed that in the as-deposited sample no CuSi phase had formed during the deposition.

⇒ In case of the annealed samples, the position of the peak corresponding to the Cu 2p photoelectrons is shifted as compared to that in the pure Cu layer.

⇒ The Cu₃Si phase formed by the annealing process.

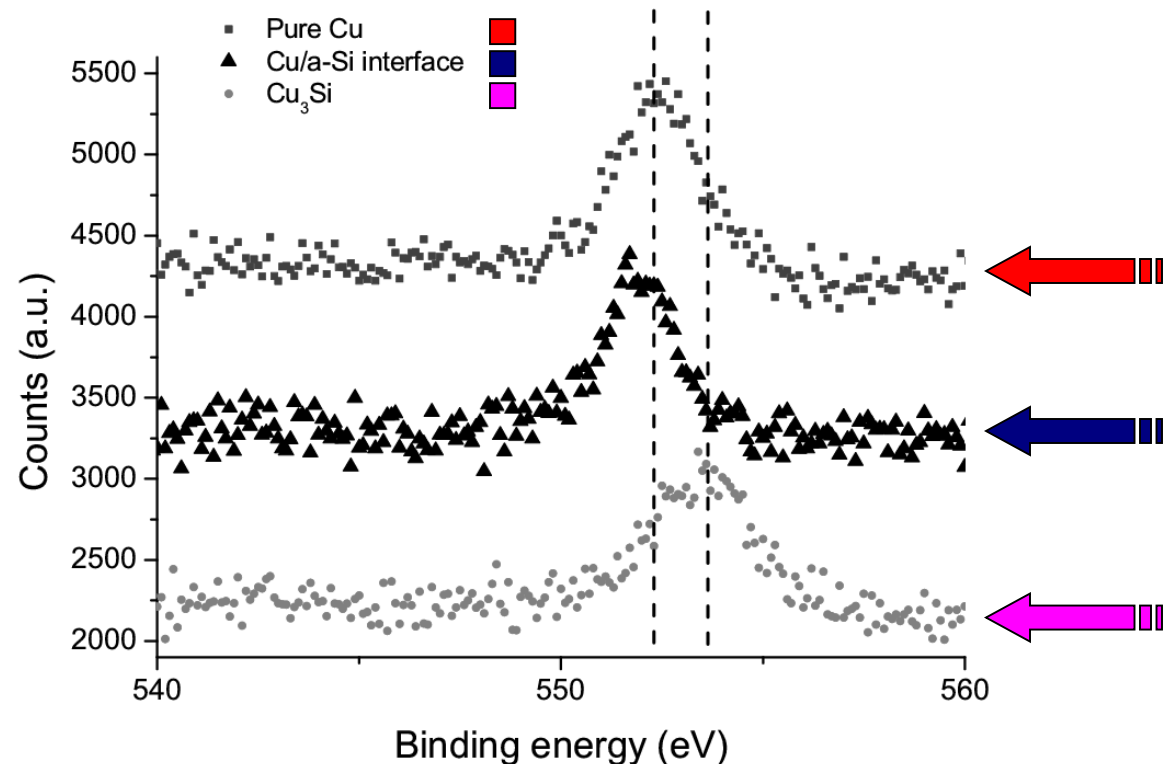


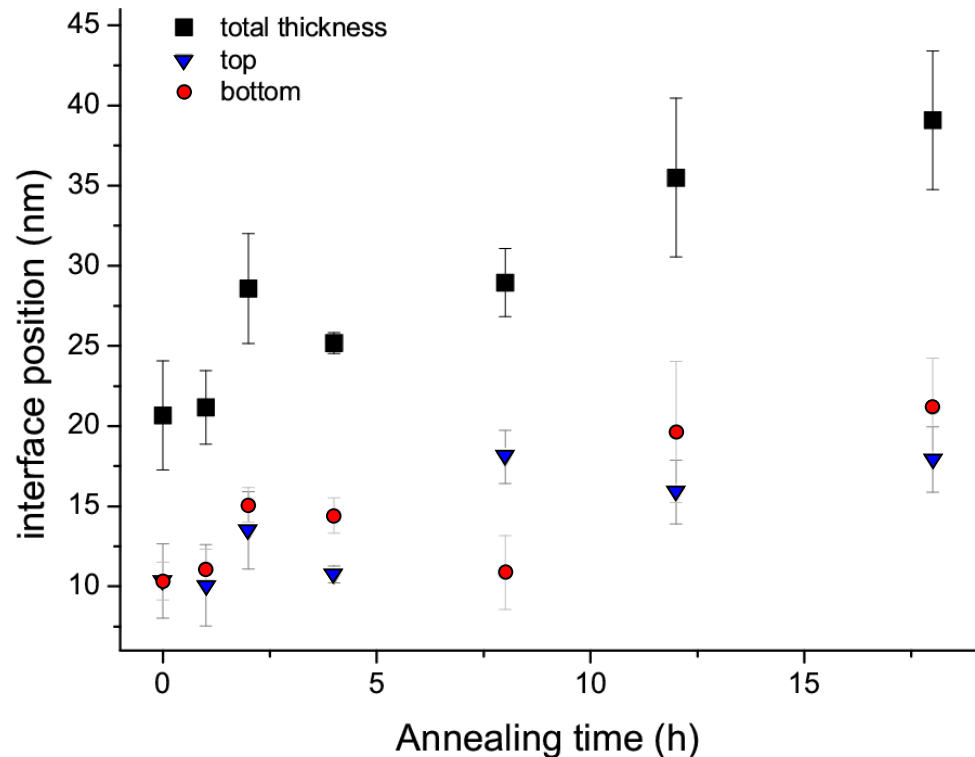
(Fig. 14. – XPS measurement results at the initial interface position before and after the heat treatment and in the pure Cu layer)

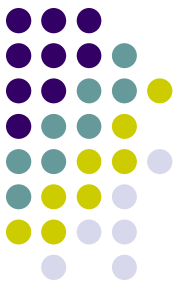
Conclusion



- ⇒ The interface positions in the function of annealing time obtained by a combination of SNMS and profilometer measurements
- ⇒ The consumption of the Si and Cu shows no real difference even though the 1:3 stoichiometry would suggest such a well measurable effect.
- ⇒ A possible explanation for this phenomenon could be the diffusion of Si into the Cu grain boundaries

(Fig. 15. – The interface position versus the annealing time, where the top and bottom means the Cu/Cu₃Si and the Cu₃Si/a-Si interface and the total equals to the thickness of the Cu₃Si layer)





- ⇒ The thickness of the Cu₃Si phases plotted versus annealing time on the logarithmic scale.
- ⇒ According to Fick's laws and the Boltzmann transformation the value of the slope should be 0.5 which one in turn correspond to square root or parabolic behavior of the phase growth.

⇒ The thickness of the growing phase is proportional to the time.

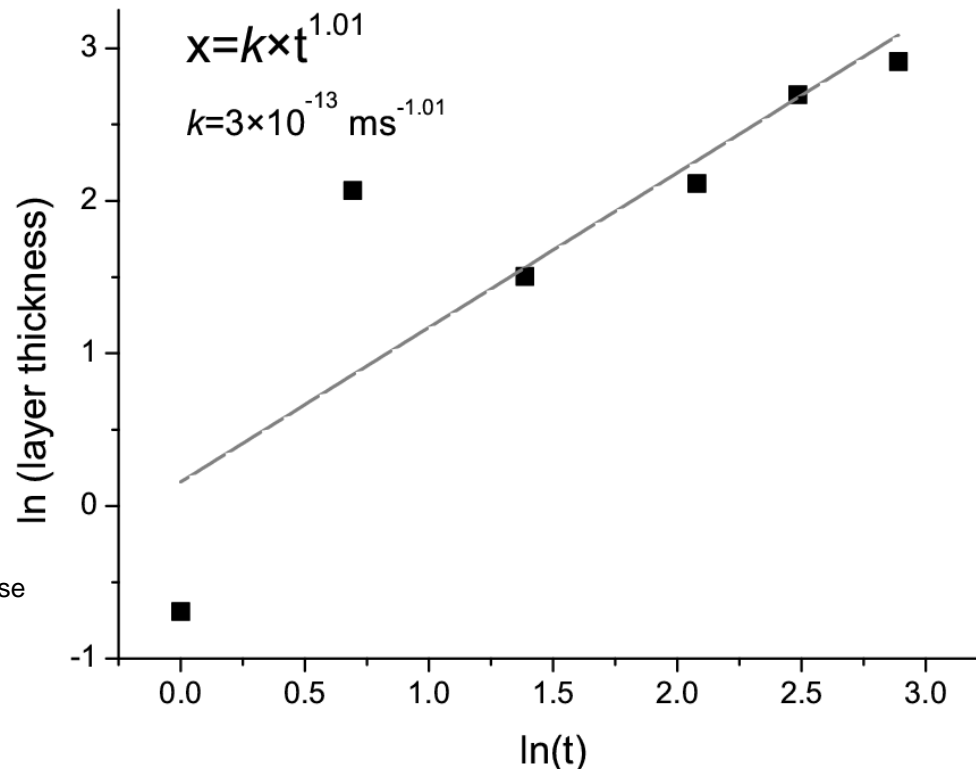
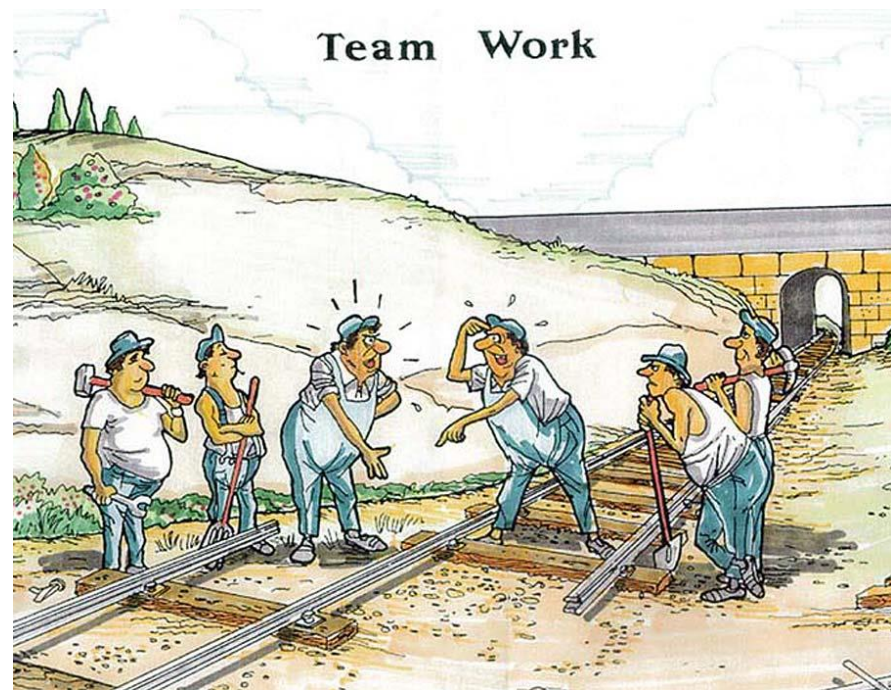


(Fig. 16. – Linear behavior of the Cu₃Si phase growth -The layer thickness on logarithmic scale versus the time on logarithmic scale)

Acknowledgements

Marianna Verezhak^{1,2}
Zoltán Balogh³
Attila Csik⁴
Gábor A. Langer¹
Dezső L. Beke¹
Guido Schmitz³
Zoltán Erdélyi¹



- 1) *Department of Solid State Physics, University of Debrecen 4026 Debrecen, Bem tér 18/b, Hungary*
- 2) *Kyiv Polytechnic Institute, National Technical University of Ukraine, 03056, Prospect Peremogy 37, Kyiv, Ukraine*
- 3) *Institute of Materials Physics, University of Münster, Wilhelm Klemmstraße 10, D-48149, Münster, Germany*
- 4) *Institute of Nuclear Research of the Hungarian Academy of Sciences (Atomki), H-4001 Debrecen, P. O. Box 51, Hungary*



Thank you for your attention!